Geochemical Journal, Vol. 40, pp. 171 to 179, 2006

Ion microprobe U-Pb dating of a dinosaur tooth

YUJI SANO,[1]* KENTARO TERADA,[2] CHI V. LY[2] and EUN JU PARK[3]

[1]Center for Advanced Marine Research, Ocean Research Institute, The University of Tokyo, Nakano-ku, Tokyo 164-8639, Japan
[2]Department of Earth and Planetary Sciences, Hiroshima University, Kagamiyama, Higashi Hiroshima 739-8526, Japan
[3]Department of Earth Science, Kyungpook National University, Sankyuk-dong, Puk-ku, Teagu, South Korea

(*Received April 15, 2004; Accepted September 6, 2005*)

Ion microprobe U-Pb dating of apatite is applied to a fossil tooth of a Allosaurid derived from the Hasandong Formation in the Gyeongsang basin, southeastern Korea. Twelve spots on a single fragment of the fossil dentine yield a Tera-Wasserburg concordia intercept age of 115 ± 10 Ma (2σ; MSWD = 0.59) on a $^{238}U/^{206}Pb$-$^{207}Pb/^{206}Pb$-$^{204}Pb/^{206}Pb$ diagram. The age provides a constraint on the depositional age of the fossil in its host Hasandong Formation as Early Aptian. The success of the ion microprobe dating depends on the heterogeneities of diagenetically incorporated U and Pb at the few hundred μm scale, the consequent variations in Pb isotopic compositions due to radioactive decay and the closed-system behavior of U and Pb. There are at least three end-members to explain the variations of minor chemical components such as FeO, SiO_2 and Al_2O_3, and trace elements such as Th, U and rare earth elements (REE) in the sample by a simple mixing model. They are (1) very low minor and REE, very high common Pb with variable U abundances, (2) low common Pb, high minor, REE, and U abundances, and (3) low minor, common Pb, and U with intermediate REE abundances, even though groups (2) and (3) may consist of a larger group. Various contributions of the three (and/or two) end-members during diagenetic prosesses may cause the elemental fractionation of U and Pb in a fossil tooth.

Keywords: fossil tooth, dinosaur, U-Pb dating, rare earth elements, diagenetic process

INTRODUCTION

In the past two decades, direct dating of sedimentary rocks has shown only limited success with Pb isotopic analyses of metamorphic carbonates (Moorbath *et al*., 1987; Jahn, 1988). This may be partly attributable to the open-system behavior of U and Pb in complex post-depositional histories such as diagenesis with U expulsion and/or Pb incorporation or exchange under the influence of pore fluids in sediment (Jahn and Cuvellier, 1994). Oxygen isotopic records suggest that apatite may be more stable and more resistant to post-depositional alteration than calcite (Karhu and Epstein, 1986). Diffusion of Pb in apatite was significantly smaller than that in calcite (Cherniak, 1997; Cherniak *et al*., 1991), suggesting a higher closure temperature and resistance to various thermal effects. Chamberlain and Bowring (2001) have reported that the apatite U-Pb thermo-chronometer is a reliable, mid-range diffusion controlled system.

Direct dating of fossilized teeth was first successfully completed by Sano and Terada (1999) using the ion microprobe ^{238}U-^{206}Pb isochron method. This technique was subsequently extended to a Carboniferous conodont via the total Pb/U isochron method (Sano and Terada, 2001) and Silurian conodonts via the ^{232}Th-^{208}Pb isochron method (Ueki and Sano, 2001). These results have convincingly shown that the U-Th-Pb isotopic systems of fossil apatite can yield credible age data with reasonable precision. The abundance of ^{238}U in small areas (about 250 μm × 250 μm) of a fossil tooth of a Permian shark has also been shown to vary significantly from 10 ppm to 100 ppm and its distribution indicates apparent coincidence with radiogenic ^{206}Pb (Sano and Terada, 1999). It has been suggested that the success of the ion microprobe dating depends on the heterogeneity of diagenetically incorporated U at the few hundred μm scale and the consequent variations in Pb isotopic compositions due to radioactive decay, since the lateral resolution of the ion microprobe method was 20~30 μm (i.e., primary beam diameter; Sano and Terada, 1999; Sano and Terada, 2001). However the mechanism to produce such chemical fractionation of U from Pb was not well understood. The primary purpose of this study is to apply the ion microprobe U-Pb dating to a tooth from a Cretaceous dinosaur and provide a constraint on the depositional age of the fossil in its host sedimentary formation. The second purpose is to provide insight into the mechanism which produces the elemental fractionation of U from Pb at the few hundred μm scale based on the chemical composition and the rare earth element (REE) abundance patterns.

*Corresponding author (e-mail: ysano@ori.u-tokyo.ac.jp)

Samples and Experimental Procedures

The sample analyzed is a fragment of a fossilized tooth of a carnivorous dinosaur (Allosaurids, Theropoda, Saurischia) which was derived from the Lower Cretaceous Hasandong Formation in the middle part of the Singdong Group, from a site about 40 km southwest of Jinju City in the Gyeongsang basin, southeastern Korea (Paik *et al*., 1998). Detailed paleontological description is given elsewhere (Park *et al*., 2000). A small fraction of the sample (approximately 12 mm × 7 mm) was cut and cast into an epoxy resin disc with a few grains of standard apatite, "PRAP", derived from an alkaline rock of the Prairie Lake circular complex in the Canadian Shield dated at 1155 ± 72 Ma (2σ; a conventional thermal ionization mass spectrometry (TIMS) ^{238}U-^{206}Pb age reported by Tilton and Kwon, 1990) and 1156 ± 45 Ma (2σ; a sensitive high resolution ion microprobe (SHRIMP) ^{207}Pb-^{206}Pb age given by Sano *et al*., 1999a). Recent measurements of PRAP have shown a SHRIMP ^{207}Pb-^{206}Pb age of 1155 ± 20 Ma (2σ; MSWD = 0.85) based on 186 spot analyses. The sample and standard were polished until their mid-sections were exposed to provide a flat surface for sputtering of secondary ions.

The sample was carbon-coated and the chemical composition and imaging of the sample was conducted by electron probe micro-analyzer (EPMA; Goldstein *et al*., 1981) to locate inclusion-free homogeneous regions (no cracks or voids) suitable for ion microprobe analysis. If there are micro-inclusions and/or secondary growth and recrystallization, they can affect the U-Pb systematics of sphene, monazite and zircon by mixed analyses (Chamberlain and Bowring, 2001). Imaging the structure of target minerals such as zircon and apatite is therefore an essential precursor to any ion microprobe analysis (Williams, 1998). Figure 1 shows an electron back-scattered image of a typical section of the sample (approximately 1.1 mm × 0.8 mm). Note that there are many cracks and voids indicated by the darker color. The tiny patches in the image are caused by heterogeneous distribution of low-atomic-number (low Z) materials and probably associated with the tubules of fossil dentine.

Prior to ion microprobe analysis, the carbon coating was removed and the mount was cleaned with petroleum spirit, detergent and pure water to reduce any surface contaminants, and was then gold-coated. The sample was kept in vacuum overnight in the sample lock of the SHRIMP II, installed at Hiroshima University, to reduce any possible hydride interference due to water absorbed onto the surface of the mount. A primary O_2^- beam of ~5 nA was focused to a 30-μm-diameter area onto each sample and/or standard and the positive secondary ions were extracted using an operating voltage of 10 kV. Before the actual analysis, the sample surface was rastered for 3 min

Fig. 1. Electron back-scattering image of a fragment of fossil tooth of a Cretaceous dinosaur, Allosaurid derived from the Hasandong Formation in the Gyeongsang basin, southeastern Korea. There are many cracks and voids indicated by dark color with low Z materials. Note that analyzed spots (TII.02 and TII.11) are located at relatively homogeneous regions.

in order to reduce the contribution of surface contaminant Pb to the analysis. No isobaric interferences were found in the mass range over ^{204}Pb and ^{208}Pb at mass resolution of 5800 using the SHRIMP II. Mercury interference on ^{204}Pb was less than 0.5% and negligibly small, which was verified by measurements of mass 200 (^{200}Hg) and 202 (^{202}Hg) (Romer, 2002; Sano and Terada, 2002). The magnet was cyclically peak-stepped from mass 159 ($^{40}Ca_2{}^{31}P^{16}O_3{}^+$) to mass 254 ($^{238}U^{16}O^+$), including the background and all Pb isotopes and masses 238 and 248 for ^{238}U and ^{232}Th^{16}O, respectively.

Identical primary beam conditions to the U-Pb measurement were used for REE analysis, while an enhanced mass resolution of 9300 at 1% peak height was adopted to separate heavy REE from oxides of light REE with adequate flat topped peaks (Sano *et al*., 1999b). The magnet was cyclically peak-stepped from mass 139 ($^{139}La^+$) to mass 175 ($^{175}Lu^+$), including the background and all significant REE isotopes ($^{140}Ce^+$, $^{141}Pr^+$, $^{145}Nd^+$, $^{146}Nd^+$, $^{147}Sm^+$, $^{149}Sm^+$, $^{151}Eu^+$, $^{153}Eu^+$, $^{155}Gd^+$, $^{157}Gd^+$, $^{159}Tb^+$, $^{161}Dy^+$, $^{163}Dy^+$, $^{165}Ho^+$, $^{166}Er^+$, $^{167}Er^+$, $^{169}Tm^+$, $^{171}Yb^+$, and $^{172}Yb^+$) and the matrix peak $^{40}Ca_2{}^{31}P^{16}O_3{}^+$. Observed intensities of the isotopes were calibrated against those of the PRAP standard whose REE contents have been determined by ICP-MS after chemical dissolution and separation elsewhere (Sano *et al*., 2002).

Results and Discussion

Observed major chemical constituents of fossil tooth dentine are listed in Table 1, and show an apparent apa-

tite signature by chemical compositions. Note that minor components such as SiO_2 and FeO contents vary significantly from 0.019% to 2.88% and 0.045% to 2.54%, respectively. There are positive correlations among various minor components (MgO, FeO, SiO_2 and Al_2O_3), while major components (CaO and P_2O_5) are depleted when minor ones are enriched. Total oxide totals yielded 93.7~97.2%, which may be partly due to Cl, F, CO_2 and rare earth elements. One explanation for the significant variation in the minor components in the sample is the result of mixed analyses that include sub-micron sized, interstitial Fe+Mn-oxyhydoxides and silicates (Kohn *et al*., 1999). It is difficult to detect ~100 nm scale clay and/or oxyhydroxide minerals by using EPMA. In the future transmission electron microscope and a high lateral resolution secondary ion mass spectrometer (Nano-SIMS, Sano *et al*., 2005) will be useful in identifying these sub-micron grains.

Table 2 lists U and Th concentrations, $^{238}U/^{206}Pb$, $^{207}Pb/^{206}Pb$, $^{204}Pb/^{206}Pb$ and $^{208}Pb/^{206}Pb$ isotope ratios of twelve spots on the sample. The $^{238}U/^{206}Pb$ ratios were obtained from the observed $^{238}U^+/^{206}Pb^+$ ratios calibrated against the PRAP apatite standard, an empirical quadratic relationship between $^{206}Pb^+/^{238}U^+$ and $^{238}U^{16}O^+/^{238}U^+$ isotope ratios and a radiometric age of 1155 ± 72 Ma (Tilton and Kwon, 1990). U and Th concentrations range from 55 ppm to 187 ppm and 2.7 ppb to 269 ppb, respectively. Note that the variation of Th is significantly larger than that of U. There is no correlation between U and Th contents where the U/Th ratios vary significantly from 254 to 45100 with an average of 12400, which is much higher than the sea water signature of about 320.

Table 1. Chemical compositions of fossil tooth of a Cretaceous dinosaur measured by EPMA

	CaO (%)	MgO (%)	FeO (%)	P_2O_5 (%)	SiO_2 (%)	Al_2O_3 (%)	Total (%)
TII.01	55.7	0.089	0.104	38.2	0.033	<0.01	94.1
TII.02	54.1	0.787	1.07	37.9	1.28	0.885	96.0
TII.03	50.5	1.65	2.32	35.8	2.88	1.87	95.1
TII.04	50.1	1.45	2.00	36.3	2.56	1.26	93.7
TII.05	56.6	0.265	0.232	38.3	0.166	0.118	95.7
TII.06	53.5	1.29	1.46	37.8	1.71	0.734	96.5
TII.07	53.9	0.691	0.928	38.0	1.13	0.685	95.3
TII.08	56.3	0.082	0.148	40.7	0.019	0.024	97.2
TII.09	56.0	0.082	0.045	39.4	0.064	<0.01	95.5
TII.10	50.0	1.56	2.54	36.1	2.58	1.67	94.5
TII.11	52.3	1.54	2.03	37.3	2.27	1.56	97.0
TII.12	53.2	1.16	1.73	37.7	1.82	1.31	96.9

Table 2. U, Th and ^{204}Pb concentrations, $^{238}U/^{206}Pb$, $^{207}Pb/^{206}Pb$, $^{204}Pb/^{206}Pb$ and $^{208}Pb/^{206}Pb$ isotopic ratios of fossil tooth of a Cretaceous dinosaur

	U (ppm)	Th (ppb)	^{204}Pb (ppm)	$^{238}U/^{206}Pb$	$^{207}Pb/^{206}Pb$	$^{204}Pb/^{206}Pb$	$^{208}Pb/^{206}Pb$
TII.01	58	217	12	0.264 ± 0.032	0.860 ± 0.020	0.0564 ± 0.0022	2.113 ± 0.064
TII.02	80	174	3.0	1.528 ± 0.214	0.860 ± 0.034	0.0562 ± 0.0018	2.129 ± 0.068
TII.03	163	5.7	0.55	12.66 ± 1.20	0.682 ± 0.022	0.0425 ± 0.0032	1.599 ± 0.052
TII.04	187	8.0	2.0	4.725 ± 0.670	0.798 ± 0.032	0.0504 ± 0.0052	1.849 ± 0.104
TII.05	66	67	0.22	12.63 ± 0.94	0.673 ± 0.020	0.0416 ± 0.0034	1.650 ± 0.334
TII.06	95	269	1.2	4.483 ± 0.832	0.801 ± 0.020	0.0542 ± 0.0032	2.034 ± 0.080
TII.07	55	42	0.23	11.23 ± 1.30	0.695 ± 0.032	0.0462 ± 0.0044	1.728 ± 0.070
TII.08	123	4.2	110	0.064 ± 0.008	0.860 ± 0.024	0.0568 ± 0.0018	2.163 ± 0.074
TII.09	106	2.7	88	0.067 ± 0.006	0.853 ± 0.024	0.0559 ± 0.0018	2.165 ± 0.068
TII.10	185	4.1	1.6	5.954 ± 0.878	0.760 ± 0.034	0.0501 ± 0.0040	1.871 ± 0.176
TII.11	95	13	0.61	7.888 ± 0.714	0.751 ± 0.014	0.0508 ± 0.0024	1.880 ± 0.034
TII.12	129	6.2	1.5	4.556 ± 0.638	0.791 ± 0.034	0.0533 ± 0.0050	1.977 ± 0.178

Error assigned to the ratio is two sigma estimated by counting statisitics and calibration. Error of U, Th and ^{204}Pb concentrations are about 30% at two sigma estimated by variations of PRAP standard.

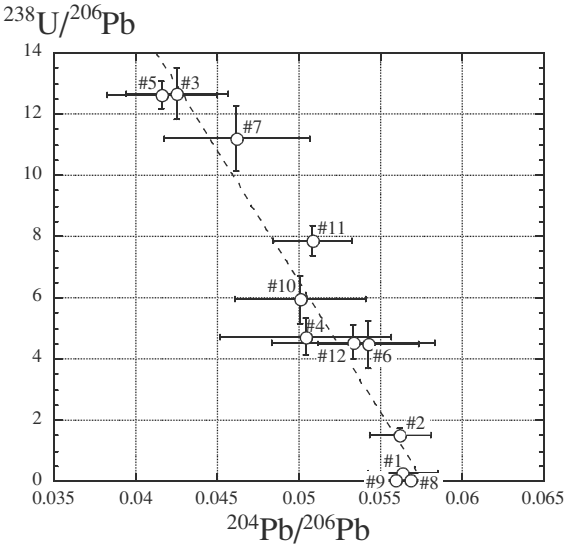

Fig. 2. A correlation diagram between $^{204}Pb/^{206}Pb$ and $^{238}U/^{206}Pb$ ratios. Errors are portrayted at the two sigma level. A dotted line shows best fit by York method. In the calculation, we take an error correlation of r = 0.

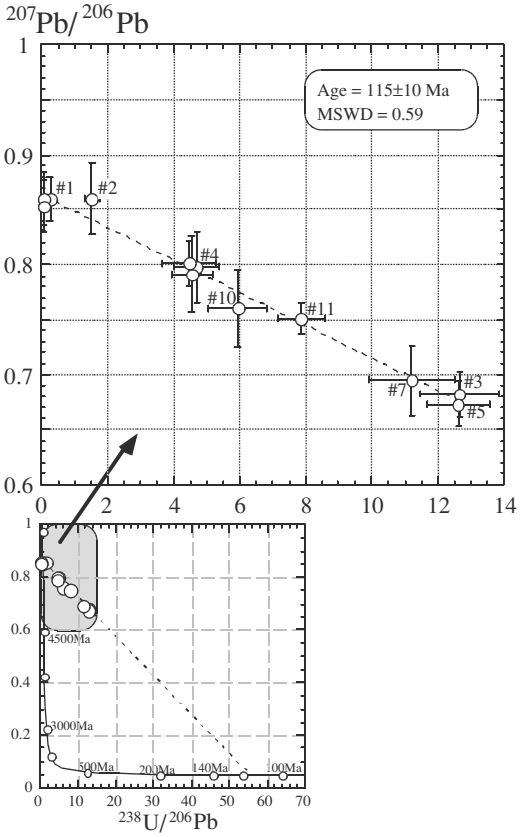

Fig. 3. Results of the three-dimensional linear regressions for the total Pb/U isochron. All data are projected on the $^{238}U/^{206}Pb$-$^{207}Pb/^{206}Pb$ plane. Errors are portrayed at the two sigma level. Linear regression (dotted line) was conducted as constrained to intersect with the Tera-Wasserburg concordia using Isoplot/Ex (Ludwig, Berkeley Geochronology Center Special Publication No. 1).

Figure 2 shows a negative correlation between the $^{204}Pb/^{206}Pb$ and $^{238}U/^{206}Pb$ isotope ratios for the fossil tooth of the Cretaceous dinosaur. A least-square fit using the York method gives the ^{238}U-^{206}Pb* isochron age of 117 ± 18 Ma (2σ *m*ean *s*quare of *w*eighted *d*eviates (MSWD) = 0.94; error correlation, rec = 0), which agrees well with the depositional age of the fossil in the Early Cretaceous (97–145.5 Ma) sedimentary sequences. All uncertainties, such as uncertainty of Pb/U ratio for standard, counting statistics, repeatability of the measurement and error propagation for data processing are taken into account to the total uncertainty. Strictly speaking, the Hasandong Formation in which the fossil tooth occurs, lies in the middle part of the Singdong Group (Paik *et al*., 1998). The Singdong Group generally has been assigned to the Hautervian (132–135 Ma) using charophytes (Seo, 1985), spores and pollen (Choi, 1985), although an early Aptian age (112–118 Ma) was suggested from paleomagnetism (Doh *et al*., 1994). The ^{238}U-^{206}Pb* age observed agrees with both Hautervian and Early Aptian ages, within the experimental uncertainty. The estimated $^{206}Pb/^{204}Pb$ ratio of common Pb is 17.54 ± 0.30 (2σ), showing less radiogenic signature than modern Pb.

Figure 3 shows the result of a three-dimensional linear regression for "total" Pb/U isochron with plotting of the $^{238}U/^{206}Pb$-$^{207}Pb/^{206}Pb$ isotopic ratios projections of all data-points (Ludwig, 1998). The calculation was made using Isoplot/Ex (Ludwig, Berkeley Geochronology Center Special Publication No. 1). The linear regressions conducted as constrained to intersect Tera-Wasserburg concordia give an age of 115 ± 10 Ma (2σ; MSWD = 0.59). This agrees well with Early Aptian, but younger than Hautervian. Since the total isochron includes all of the information from the $^{238}U/^{206}Pb$-$^{204}Pb/^{206}Pb$, $^{207}Pb/^{206}Pb$-$^{204}Pb/^{206}Pb$ and $^{238}U/^{206}Pb$-$^{207}Pb/^{206}Pb$ isotopic ratios at once, a small MSWD suggests the high probability of fitting and no detectable open-system or variable-initial-ratio behavior. The ion microprobe results confirm that the depositional age of the Singdong Group is Early Aptian. The initial $^{206}Pb/^{204}Pb$ and $^{207}Pb/^{204}Pb$ ratios were determined from the intersection of the regression line with the $^{207}Pb/^{206}Pb$-$^{204}Pb/^{206}Pb$ plane. Values of 17.56 ± 0.25 (2σ), for $^{206}Pb/^{204}Pb$, and 15.15 ± 0.25 (2σ), for $^{207}Pb/^{204}Pb$ were obtained, which give a negative age on the Stacey-Kramer two-stage growth curve (Stacey and Kramers, 1975), similar to the common Pb observed in the fossilized tooth of a Permian Shark (Sano and Terada, 1999). This is probably due to those frequently found

Table 3. Rare earth element abundances in fossil tooth of a Cretaceous dinosaur together with sum REE, Ce/Ce, Eu/Eu* and Lu/La ratios*

	TII.03 (ppm)	TII.06 (ppm)	TII.09 (ppm)	TII.10 (ppm)
La	2610 ± 780	340 ± 100	37 ± 11	880 ± 270
Ce	4800 ± 1400	420 ± 130	23 ± 7	1220 ± 370
Pr	560 ± 170	33 ± 10	2.0 ± 0.6	124 ± 37
Nd	2390 ± 720	104 ± 31	7.6 ± 2.3	460 ± 140
Sm	520 ± 160	21 ± 6	1.7 ± 0.5	94 ± 28
Eu	270 ± 81	7.1 ± 2.1	0.47 ± 0.14	43 ± 13
Gd	600 ± 180	19 ± 6	1.6 ± 0.5	104 ± 31
Tb	81 ± 24	2.5 ± 0.7	0.29 ± 0.09	15 ± 5
Dy	360 ± 110	11 ± 3	2.4 ± 0.7	71 ± 21
Ho	58 ± 17	1.8 ± 0.5	0.71 ± 0.21	13 ± 4
Er	137 ± 41	4.4 ± 1.3	2.6 ± 0.8	32 ± 10
Tm	16 ± 5	0.57 ± 0.17	0.46 ± 0.14	4.1 ± 1.2
Yb	71 ± 21	3.3 ± 1.0	3.3 ± 1.0	21 ± 6
Lu	8.6 ± 2.6	0.47 ± 0.14	0.56 ± 0.17	2.5 ± 0.8
sum REE	12500 ± 3800	970 ± 290	84 ± 25	3100 ± 900
Ce/Ce*	1.00 ± 0.30	0.99 ± 0.30	0.67 ± 0.20	0.92 ± 0.28
Eu/Eu*	2.20 ± 0.70	1.60 ± 0.48	1.29 ± 0.39	1.98 ± 0.60
Lu/La	0.22 ± 0.07	0.09 ± 0.03	1.01 ± 0.30	0.19 ± 0.06

Errors of REE concentrations are at two sigma estimated by 5-6 successive measurements of standard apatite, PRAP (Sano et al., 2002).

anomalous Pb in some ore deposits with mixing of the single-stage Pb and varying amounts of radiogenic Pb derived from U and Th-bearing minerals in the crust (Sinclair, 1966).

The success of the in situ ion microprobe U-Pb dating of fossil tooth fragments depends on the chemical fractionation of diagenetically incorporated U from common Pb at the few hundred-μm scale in the sample (cf., a contour map of ^{238}U concentration in small section, 250 μm × 250 μm of the fossil tooth from figure 1 of Sano and Terada, 1999), the consequent variations in Pb isotopic compositions due to radioactive decay of U and the closed-system behavior of U and Pb. Incorporation of U in fossil tooth may have completed within 100 ka (Williams and Marlow, 1987) as discussed latter. The time elapsed is significantly shorter than the error of the total Pb/U isochron age of ±10 Ma. Diffusion of radiogenic Pb in apatite at low temperature during the geological time is significantly slow (Cherniak *et al*., 1991). These lines of evidences may justify the ion microprobe U-Pb age.

It is well documented that U, Th and REE are not taken up by living animal teeth (Elderfield and Pagett, 1986; Veeh, 1982). These elements may have been enriched in the tooth during early diagenetic processes either by chemical alteration of the original apatite crystals or incorporation of ~100 nm scale clay particles and oxyhydroxide mineral (Kohn *et al*., 1999). It is also documented that buried bone takes up large amounts of U and the U content increases with the duration of burial and the local groundwater concentration of U (Williams and Marlow, 1987; Badone and Farquar, 1982). Generally bones buried for longer than 100 ka are fairly uniform in the spatial distribution of U (Williams and Marlow, 1987), while those buried for shorter periods exhibit a concentration gradient decreasing from the outer surface (Badone and Farquar, 1982). A diffusion-adsorption model of U uptake by archaeological bone has been proposed (Millard and Hedges, 1996) and may be applicable to tooth dentine since the structure of dentine is basically similar to that of bone. In addition bone has essentially the same chemistry as tooth dentine. Uranyl ions (UO_2^{2+}) and their complexes in groundwater and pore fluids in sediment may diffuse and are adsorbed on the internal surface of the dentine because of the high affinity of hydroxyapatite for uranyl ions. Changes in dentine structure (increase of crystallinity and growth of fracolite and other minerals filling the space formerly occupied by organic matter during diagenesis) may bind U in the mineral structure. At the same time, incorporation of ~100 nm scale clay particles and oxyhydroxide mineral may also occur.

In order to discuss the diagenetic mechanism of the fossil, all REE abundances were measured at four spots where U and Pb were previously analyzed. Table 3 lists REE concentrations together with total REE abundance (sum REE), Ce/Ce*, Eu/Eu* and Lu/La ratios, where Ce*

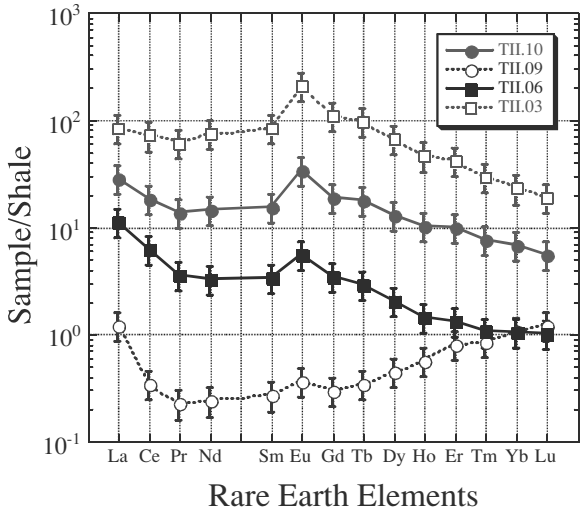

Fig. 4. Shale-normalized rare earth abundance patterns of three spots on the fragment of fossil tooth of Cretaceous dinosaur, Allosaurids, Theropoda, Saurischia. Errors are portrayed at the two sigma level.

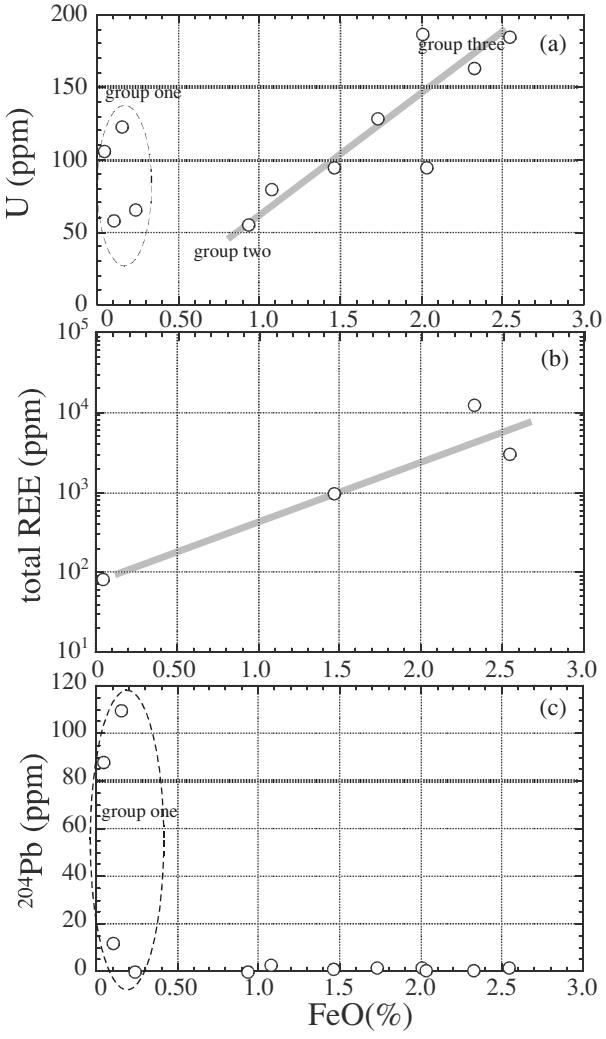

Fig. 5. A correlation diagram between (a): FeO (%) and U (ppm) concentrations in the sample fossil. (b): A comparison between FeO (%) and total REE (ppm) concentrations. (c): A comparison between FeO (%) and ^{204}Pb (ppm). Note that high ^{204}Pb contents are observed at relatively pure apatite region where MgO and SiO_2 are also depleted.

and Eu* are calculated by $La^{1/2} \times Pr^{1/2}$ and $Sm^{1/2} \times Gd^{1/2}$ in the shale normalized pattern (Gromet *et al*., 1984). The contents vary significantly from less than 1 ppm of heavy REE to ~5000 ppm of light REE. Figure 4 shows the shale-normalized REE patterns of four spots on the sample. The REE patterns resemble each other except for the TII.09 spot, having a broadly flat pattern from light REE to middle REE and a decrease from middle REE to heavy REE except for an apparent positive anomaly at Eu. The REE pattern of the TII.09 is distinctive from the others with a feature of generally smaller abundance of REE, the increase from Pr to Lu, and smaller Eu positive anomaly.

These REE patterns are similar to those of old biogenic apatite such as Carboniferous conodont (Sano and Terada, 2001) while they are distinguished from Fransian-Famennian (Grandjean-Lecuyer *et al*., 1993) and Silurian (Ueki and Sano, 2001) conodonts, which have a concave-shape pattern of middle REE enrichment. The difference was attributed to either redox state changes during the diffusive exchange of REE or different formation environments, such as river and seawater (Sano and Terada, 2001). Based on the REE study of Cambrian phosphorites, Shields and Stille (2001) have reported that post-depositional alteration may tend to (1) increase REE contents, (2) reverse Ce depletion, (3) alter Eu anomalies, and (4) concentrate preferentially the middle REE. If this is the case in the present sample, the change of REE pattern from TII.09 to TII.10 through TII.10 and TII.03 may be explained by the result of progressive REE scavenging after deposition. We do not discuss the redox state changes because the Ce anomalies are small and probably within the experimental error margin.

There are significant positive correlations among minor chemical components such as FeO and Al_2O_3 (see Table 1). Their coefficients are as follows: FeO-SiO_2 (r^2 = 0.977); FeO-MgO (r^2 = 0.969); MgO-Al_2O_3 (r^2 = 0.917); Al_2O_3-SiO_2 (r^2 = 0.945). Therefore one can select the FeO abundance as a representative of minor components. Figure 5a shows a correlation between U and FeO contents in the fossil tooth. There is a positive correlation between them except for the samples whose FeO concentrations are less than 0.5% (defined here by a group one). Samoilov and Smirnova (2000) have reported that carbonate-fluorapatite formed as a result of the substitution of biogenic

hydroxy-apatite and organic bone phosphate during the early diagenetic fossilization of dinosaur bone remains with the enrichment of diagenetic apatite in Si, S, C, F, Na, REE, Y, Sr and Ba. The trend except for group one is consistent with the results of Shields and Stille (2001) and shows a possible mechanism for tooth diagenesis. The positive correlation ($r^2 = 0.735$) between U and FeO (excluding group one) may be attributable to the concurrent incorporation of these elements into the tooth by the chemical alteration of the original apatite crystals or incorporation of ~100 nm scale clay particles and oxyhydroxide mineral. Group two is characterized by relatively low minor and REE abundances, while group three shows high minor and REE abundances. On the other hand, groups two and three may be end-members of one large group, which is supported by a positive correlation between FeO and U contents in Fig. 5a. Figure 5b indicates a positive correlation between FeO and total REE abundances in the fossil tooth. The trend is again consistent with the idea of diagenetic enrichment of REE in dinosaur bone reported by Samoilov and Smirnova (2000).

On the other hand, the uptake mechanism of Pb in tooth and/or bone may be different from that of U. It is well known that Pb enters the body primarily via ingestion and secondarily through inhalation (Doull *et al*., 1980; Needlman and Landrigan, 1981). Pb then contaminates the blood and various organs are affected. Bloch *et al*. (1998) suggested that Pb is accumulated and immobilized for long periods of time in teeth and that Pb contents can be used as an indicator of the cumulative Pb intake of a human child. Stern *et al*. (1999) reported that it is possible to reconstruct Pb isotope exposure history preserved in the growth layers of Walrus teeth using SHRIMP. They further suggested the idea of using the tooth annuli of animals as reliable archives of environmental Pb exposure.

Figure 5c shows the relationship between FeO and ^{204}Pb (indicator of common Pb) concentrations in the fossil tooth. Note that ^{204}Pb is enriched at the site of pure apatite signatures (group one) where minor elemental abundances are significantly small. The relation suggests that group one did not chemically behave like the other samples (group two and three) where U abundances are correlated with FeO. Estimated common Pb in the sample has a ^{206}Pb/^{204}Pb ratio of 17.56 and ^{207}Pb/^{204}Pb ratio of 15.15, and a correlation between ^{204}Pb/^{208}Pb and ^{232}Th/^{208}Pb ratios gives a common ^{208}Pb/^{204}Pb ratio of 37.76. From this a total Pb/^{204}Pb ratio of ~71.5 was calculated, from which a value for gross common Pb based on ^{204}Pb concentration can be obtained. The common Pb contents of the dinosaur tooth was found to vary significantly from 16 ppm to 7860 ppm with an average of 1320 ppm, which is extraordinary high when compared with those of ~10 ppm in a fossilized tooth of a Permian shark (Sano and Terada, 1999), ~0.5 ppm in Carboniferous conodont (Sano and Terada, 2001), ~2 ppm in the growth layers of Walrus teeth (Stern *et al*., 1999) and ~50 ppm of shed teeth of contemporary human children in Pb polluted environments (Bloch *et al*., 1998). Such high Pb abundance has not been reported via ingestion or inhalation. Molleson *et al*. (1998) reported an extreme case of human bone diagenesis from lead-lined coffins at Christ Church in London. Chemical analyses of the bone showed Pb contents of up to 37%, which was due to post-mortem alteration and re-crystallization of bone, in the presence of solutions rich in Pb, over a period of less than 200 years.

Based on the abundances of minor and trace elements in the fossil tooth, there are at least three end-members to explain the variations of chemical components in the sample by a simple mixing model. Group one has very low minor and REE, very high common Pb with variable U abundances, while groups two and three are characterized by low common Pb, high minor, REE, and U abundances, and low minor, common Pb, and U with intermediate REE abundances, respectively, even though groups two and three may simply consist of a large group. Variable contributions of the three (and/or two) end-members during diagenetic processes may cause the elemental fractionation of U and Pb in a fossil tooth. Further work is needed to understand such phenomena.

CONCLUSIONS

Ion microprobe U-Pb dating of a fossil tooth of a carnivorous dinosaur (Allosaurids, Theropoda, Saurischia) has identified its host Hasandong Formation as Early Aptian, 115 ± 10 Ma (95%CL). The chemical compositions of minor and trace elements and REE abundance patterns reveal that there may be at least three end-members. Trace elements such as U, REE and minor elements were diagenetically incorporated in the tooth after the remains were deposited, while the mechanism to uptake the common Pb may be different from those of U and REE. Large common Pb abundance, ~0.8% in the tooth, suggests an extreme case of tooth diagenesis.

Acknowledgments—We thank A. Kano, S. Ueki and Y. Shibata for discussions and technical support. We appreciate K. R. Ludwig and R. L. Romer for helpful comments on the linear regressions for a total Pb/U isochron and the Hg interference on ^{204}Pb in fossil apatite, respectively. An earlier version of the paper was peer reviewed by K. R. Ludwig. Constructive reviews of two anonymous referees were useful to improve the manuscript greatly. This is a contribution of joint project between SHRIMP laboratory at Hiroshima University and Center for Advanced Marine Research at Ocean Research Institute, The University of Tokyo.

References

Badone, E. and Farquar, R. M. (1982) Application of neutron activation analysis to the study of element concentration and exchange in fossil bones. *J. Radioanalyt. Chem.* **69**, 291–311.

Bloch, P., Shapiro, I. M., Soule, L., Close, A. and Revich, B. (1998) Assessment of lead exposure of children from K-XRF measurements of shed teeth. *App. Rad. Isot.* **49**, 703–705.

Chamberlain, K. R. and Bowring, S. A. (2001) Apatite-feldpar U-Pb thermochronometer: a reliable, mid-range (similar to 450 degree C), diffusion-controlled system. *Chem. Geol.* **172**, 173–200.

Cherniak, D. J. (1997) An experimental study of strontium and lead diffusion in calcite, and implications for carbonate diagenesis and metamorphism. *Geochim. Cosmochim. Acta* **61**, 4173–4179.

Cherniak, D. J., Lanford, W. and Ryerson, F. J. (1991) Lead diffusion in apatite and zircon using ion implantation and Rutherford Backscattering techniques. *Geochim. Cosmochim. Acta* **58**, 1663–1673.

Choi, D. K. (1985) Spores and pollen from the Gyeongsang Supergroup, southeastern Korea and their chronologic and paleoecologic implications. *J. Paleontol. Soc. Korea* **21**, 33–50.

Doh, S. J., Hwang, C. S. and Kim, K. H. (1994) A paleomagnetic study of sedimentary rocks from Kyeongsang Supergroup in Milyang Subbasin. *J. Geol. Soc. Korea* **30**, 211–228.

Doull, J., Klaassen, C. D. and Amdur, M. O. (1980) *Toxicology: The Basic Science of Poisons*. Macmillan, New York.

Elderfield, H. and Pagett, R. (1986) REE in ichthyoliths: Variations with redox conditions and depositonal environment. *Sci. Total Env.* **49**, 175–197.

Goldstein, J. I., Newbury, D. E., Echlin, P., Joy, D. C., Fiori, C. and Lifshin, E. (1981) *Scanning Electron Microscopy and X-ray Microanalysis*. Plenum Press, New York, 673 pp.

Grandjean-Lecuyer, P., Feist, R. and Albarede, F. (1993) Rare earth elements in old biogenic apatites. *Geochim. Cosmochim. Acta* **57**, 2507–2514.

Gromet, L. P., Dymek, R. F., Haskin, L. A. and Korotev, R. L. (1984) The North American Shale Composite: Compilation, major and trace-element characteristics. *Geochim. Cosmochim. Acta* **48**, 2469–2482.

Jahn, B. M. (1988) Pb-Pb dating of young marbles from Taiwan. *Nature* **332**, 429–432.

Jahn B. M. and Cuvellier, H. (1994) Pb-Pb and U-Pb geochronology of carbonate rocks: an assessment. *Chem. Geol.* **115**, 125–151.

Karhu, J. and Epstein, S. (1986) The implication of the oxygen isotope records in coexisting cherts and phosphates. *Geochim. Cosmochim. Acta* **50**, 1745–1756.

Kohn, M. J., Schoeninger, M. J. and Barker, W. W. (1999) Altered status: Effects of diagenesis on fossil tooth chemistry. *Geochim. Cosmochim. Acta* **63**, 2737–2747.

Ludwig, K. (1998) On the treatment of concordant uranium-lead ages. *Geochim. Cosmochim. Acta* **62**, 665–676.

Millard, A. R. and Hedges, R. E. M. (1996) A diffusion-adsorption model of uranium uptake by archaeological bone. *Geochim. Cosmochim. Acta* **60**, 2139–2152.

Molleson, T. I., Willaims, C. T., Cressey, G. and Din, V. K. (1998) Radiographically opaque bones from lead-lined coffins at Christ Church, Spitalfields, London—an extreme example of bone diagenesis. *Bull. Soc. Geol. France* **169**, 425–432.

Moorbath, S., Taylor, P. N., Orpen, J. L., Treloar, P. and Wilson, J. F. (1987) First direct radiometric dating of Archaean stromatolite limestone. *Nature* **326**, 865–867.

Needlman, H. L. and Landrigan, P. J. (1981) The Health Effects of low level exposure to lead. *Ann. Rev. Public Health* **2**, 277–298.

Paik, I. S., Lee, Y. I., Lee, Y. U., Cheong, D. K. and Kimm, S. J. (1998) Dinosaur beds in the Cretaceous Hasandong Formation in the vicinity of Jinju City, Gyeongnam, Korea. *J. Paleont. Soc. Korea* **14**, 14–32.

Park, E. J., Yang, S. Y., and Currie, P. J. (2000) Early Cretaceous Dinosaur teeth of Korea. *J. Paleont. Soc. Korea Special Publication* **4**, 85–98.

Romer, R. L. (2002) Comment on "In situ ion microprobe U-Pb dating and REE abundances of a Carboniferous conodont". *Geophys. Res. Lett.* **29**, 12, 38.

Samoilov, V. S. and Smirnova, E. V. (2000) Apatite from dinosaur bone remains (the Gobi Desert, south Mongolia). *Neues Jahrbuch Fru Mineralogie-Monautshefte* **3**, 129–144.

Sano, Y. and Terada, K. (1999) Direct ion microprobe U-Pb dating of fossil tooth of a Permian shark. *Earth Planet. Sci. Lett.* 174, 75–80.

Sano, Y. and Terada, K. (2001) In situ ion microprobe U-Pb dating and REE abundances of a Carboniferous conodont. *Geophys. Res. Lett.* **28**, 831–834.

Sano, Y. and Terada, K. (2002) Reply to Romer. *Geophys. Res. Lett.* **29**, 12, 39.

Sano, Y., Oyama, T., Terada, K. and Hidaka, H. (1999a) Ion microprobe U-Pb dating of apatite. *Chem. Geol.* **153**, 249–258.

Sano, Y., Terada, K., Hidaka, H., Nishio, Y., Amakawa, H. and Nozaki, Y. (1999b) Ion-microprobe analysis of rare earth elements in oceanic basalt glass. *Anal. Sci.* **15**, 743–748.

Sano, Y., Terada, K. and Fukuoka, T. (2002) High mass resolution ion microprobe analysis of rare earth elements in silicate glass, apatite and zircon: lack of matrix dependency. *Chem. Geol.* **184**, 217–230.

Sano, Y., Shirai, K., Takahata, N., Hirata, T. and Sturchio, N. C. (2005) Nano-SIMS Analysis of Mg, Sr, Ba and U in Natural Calcium Carbonate. *Anal. Sci.* **21**, 1091–1097.

Seo, S. J. (1985) Lower Cretaceous geology and paleontology (Charophyta) of central Gyeongsang Basin, South Korea. Unpublished Ph.D. Thesis, Kyungbuk National University, 177 pp.

Shields, G. and Stille, P. (2001) Diagenetic constraints on the use of cerium anomalies as palaeoseawater redox proxies: an isotopic and REE study of Cambrian phosphorites. *Chem. Geol.* **175**, 29–48.

Sinclair, A. J. (1966) Anomalous lead from the Kootenay Arc, British Columbia. *A Symposium on the Tectonic History and Mineral Deposits of the Western Cordillera*, Vancouver, Can. Inst. Min. and Metal. Spec. Vol. 8, 249–262.

Stacey, J. S. and Kramers, J. D. (1975) Approximation of ter-

restrial lead isotope evolution by a two-stage model. *Earth Planet. Sci. Lett.* **26**, 207–221.

Stern, R. A., Outridge, P. M., Davis, W. J. and Stewart, R. E. A. (1999) Reconstructing lead isotope exposure histories preserved in the growth layers of walrus teeth using the SHRIMP II ion microprobe. *Environ. Sci. Technol.* **33**, 1771–1775.

Tilton, G. R. and Kwon, S.-T. (1990) Isotopic evidence for crust-mantle evolution with emphasis on the Canadian Shield. *Chem. Geol.* **83**, 149–163.

Ueki, S. and Sano, Y. (2001) In situ ion microprobe Th-Pb dating of Silurian conodonts. *Geochem. J.* **35**, 307–314.

Veeh, H. H. (1982) Concordant ^{230}Th and ^{231}Pa ages of marine phosphorites. *Earth Planet. Sci. Lett.* **57**, 278–284.

Williams, C. T. and Marlow, C. A. (1987) Uranium and thorium distributions in fossil bones from Olduvai Gorge, Tanzania and Kanam, Kenya. *J. Archaeol. Sci.* **14**, 297–309.

Williams, I. S. (1998) U-Th-Pb geochronology by ion microprobe. *Reviews in Economic Geology* **7**, 1–35.